Int. J. Heat Mass Transfer. Vol. 34, No. 1, pp. 237–246, 1991
Printed in Great Britain

0017–9310/91 $3.00+0.00

Natural convection in a partially divided rectangular enclosure with an opening in the partition plate and isoflux side walls

K. S. CHEN† and P. W. KO
Department of Mechanical Engineering, National Sun Yat-Sen University, Kaohsiung, Taiwan, R.O.C.

(*Received* 16 *October* 1989 *and in final form* 27 *February* 1990)

Abstract—A numerical study is presented for natural convection in a two-dimensional, partially-divided, rectangular enclosure in which two side walls were maintained at uniform heat flux condition and the top and bottom walls were insulated. The modified Rayleigh number ranging from 10^4 to 10^8, the opening ratios of 0, 1/4, 1/8 and 1/2, and the conductivity ratios 0.02, 1 and 50 were investigated for an enclosure aspect ratio (length/height) of 2, partition ratio of 1/2 and Prandtl number of 7 (for water). Results show that the hot fluid flowed to the other side of the enclosure mainly through the bottom of the partition when there was no opening in the partition, and a weak circulation zone was present in the upper and left quadrant. With an opening in the partition, most of the fluid flowed to the other side through the opening and the circulation zone in the upper and left quadrant was reduced in size or disappeared. The effect of partition conductivity on the heat transfer rate was found rather small and could be neglected. Correlation of the average Nusselt number in terms of the modified Rayleigh number and the opening ratio was obtained and discussed. Results also show that an unopened partial obstruction would reduce the heat transfer rate by 12–44% depending on the modified Rayleigh number.

1. INTRODUCTION

NATURAL convective motion in simple enclosures with differentially heated vertical walls has received considerable attention in the past, due to its important applications relating to the solar collector design, cooling of electronic components, fire spread and energy transfer in rooms and buildings, cooling of nuclear reactors and the growth of single crystals from crucible melts. Comprehensive reviews on the heat transfer pertaining to the enclosures have been summarized recently in refs. [1–4].

On many occasions, natural convection in complex enclosures, such as a partial obstruction extending downward from the ceiling or upward from the floor, is also important. This geometry corresponds to a printed circuit board in an electronic cabinet, or a ceiling beam in a room, and has received attention recently; see refs. [5–15]. It was found that a weak circulation zone in the upper quadrant near the hot wall [10, 11] or a weak circulation zone in the lower quadrant near the cold wall [12] was responsible for reducing the heat transfer across the enclosure. The experimental study by Chen *et al.* [16] showed that if there was a slot or an opening in the partition plate the weak recirculation zone disappeared and the heat transfer rate increased with increasing opening size. However, the work described by Chen *et al.* [16] was mainly for an 'isothermal wall' condition and a non-conducting partition plate. In addition, it has been argued that in many situations the 'uniform heat flux' condition on the two side walls is a more appropriate model for the enclosure convection; see Kimura and Bejan [17].

The objective of this study is to document the natural convective flow and heat transfer characteristics in a two-dimensional rectangular enclosure both with and without an opening in the partition plate under isoflux condition on the two side walls. The numerical simulation was carried out for an enclosure with an aspect ratio of $A = L/H = 2$ and a partition ratio of $A_p = h/H = 1/2$ with water ($Pr = 7$) as the working fluid. Effects of the opening size, the modified Rayleigh number and the conductivity ratio on the flow and heat transfer behaviours are examined and discussed.

2. GOVERNING EQUATIONS AND SOLUTION PROCEDURES

Consider a two-dimensional rectangular enclosure filled with fluid, such as is shown in Fig. 1. The uniform heat flux is specified along the two side walls, and the top and bottom walls are insulated. The partition plate, with a height $h = H/2$ and a thickness $w = 0.01H$, is placed in the middle of the top wall and protrudes downward into the enclosure. The opening with size s is located in the middle of the partition plate. Employing the Boussinesq approximation, the

† Author to whom all correspondence should be addressed.

NOMENCLATURE

A	aspect ratio, L/H
A_o	opening ratio, s/H
A_p	partition ratio, h/H
g	gravitational acceleration
H	enclosure height, see Fig. 1
h	height of partition plate, see Fig. 1
k_f	thermal conductivity of the fluid
k_p	thermal conductivity of the partition plate
k_r	conductivity ratio, k_p/k_f
L	enclosure length, see Fig. 1
Nu	average Nusselt number defined in equation (9)
Nu_y	local Nusselt number defined in equation (8)
P	non-dimensional pressure, $(p-p_\infty)/(\rho\alpha^2/H^2)$
p	local fluid pressure
Pr	Prandtl number of the fluid, ν/α
p_∞	ambient pressure
q	uniform wall heat flux on the side wall
Ra	Rayleigh number, $g\beta(T_h-T_c)H^3/(\nu\alpha)$
Ra^*	modified Rayleigh number, $g\beta qH^4/(\nu\alpha k_f)$
s	opening size, see Fig. 1
T	temperature
T_c	local temperature of cold wall
T_h	local temperature of hot wall
u	horizontal velocity component
U	non-dimensional horizontal velocity component, uH/α
v	vertical velocity component
V	non-dimensional vertical velocity component, vH/α
x	horizontal coordinate
X	non-dimensional horizontal coordinate, x/H
y	vertical coordinate
Y	non-dimensional vertical coordinate, y/H.

Greek symbols

α	thermal diffusivity of the fluid
β	thermal expansion coefficient of the fluid
Δ	difference
θ	non-dimensional temperature difference, $(T-T_\infty)/(qH/k_f)$
μ	dynamic viscosity of the fluid
ν	kinematic viscosity of the fluid, μ/ρ
ρ	fluid density.

Subscript

∞	ambient condition.

non-dimensional equations describing the steady and laminar flow are

$$\frac{\partial U}{\partial X}+\frac{\partial V}{\partial Y}=0 \quad (1)$$

$$U\frac{\partial U}{\partial X}+V\frac{\partial U}{\partial Y}=-\frac{\partial P}{\partial X}+Pr\left(\frac{\partial^2 U}{\partial X^2}+\frac{\partial^2 U}{\partial Y^2}\right) \quad (2)$$

$$U\frac{\partial V}{\partial X}+V\frac{\partial V}{\partial Y}=-\frac{\partial P}{\partial Y}+Pr\left(\frac{\partial^2 V}{\partial X^2}+\frac{\partial^2 V}{\partial Y^2}\right)+Ra^*\,Pr\,\theta \quad (3)$$

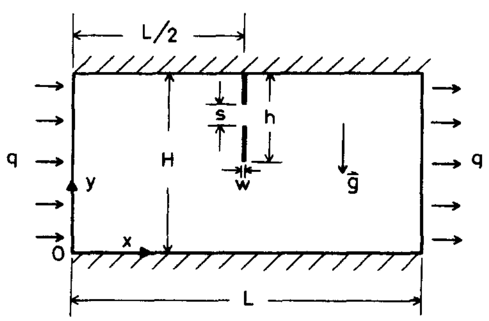

FIG. 1. Partially divided enclosure with an opening in the partition plate and isoflux condition on the side walls.

$$U\frac{\partial \theta}{\partial X}+V\frac{\partial \theta}{\partial Y}=\frac{\partial^2 \theta}{\partial X^2}+\frac{\partial^2 \theta}{\partial Y^2}. \quad (4)$$

The temperature distribution inside the plate is given by

$$\frac{\partial^2 \theta}{\partial X^2}+\frac{\partial^2 \theta}{\partial Y^2}=0. \quad (5)$$

The boundary conditions along the four walls are

$$X=0:\quad U=V=0,\quad \frac{\partial \theta}{\partial X}=-1 \quad (6a)$$

$$X=1:\quad U=V=0,\quad \frac{\partial \theta}{\partial X}=-1 \quad (6b)$$

$$Y=0:\quad U=V=0,\quad \frac{\partial \theta}{\partial Y}=0 \quad (6c)$$

$$Y=1:\quad U=V=0,\quad \frac{\partial \theta}{\partial Y}=0. \quad (6d)$$

The no-slip conditions are also satisfied on the partition plate, and the energy balance at the fluid–partition interface requires

$$\left(-\frac{\partial \theta}{\partial n}\right)_{\text{fluid}}=\left(-k_r\frac{\partial \theta}{\partial n}\right)_{\text{partition}} \quad (7)$$

where n is a unit vector normal to the interface surface.

In this study the enclosure aspect ratio $A(=2)$, the partition ratio $A_p(=1/2)$, the partition width

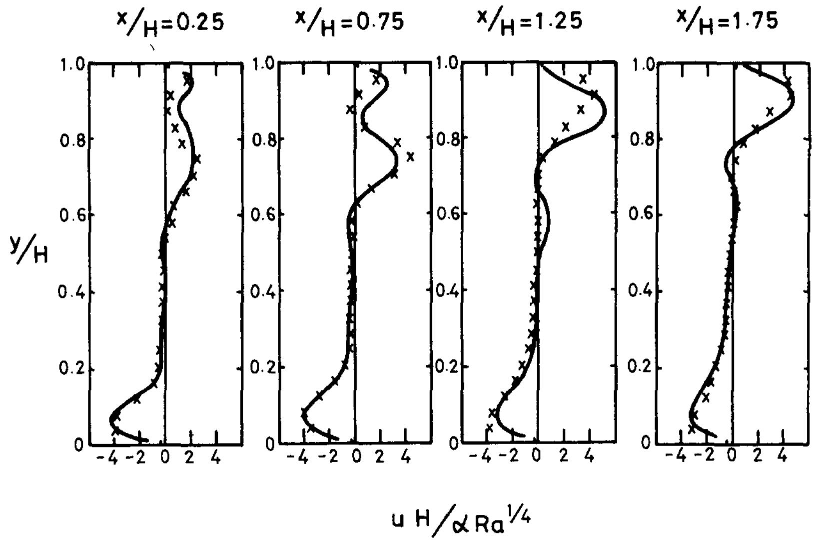

FIG. 2. Comparison of velocity profiles: ——, calculation; ×, from ref. [16].

$w/H(=0.01)$ and the Prandtl number $Pr(=7)$ were kept constant. Numerical simulations were carried out for the modified Rayleigh number (Ra^*) ranging from 10^4 to 10^8, the opening ratios ($A_o = s/h$) of 0, 1/8, 1/4 and 1/2, and the conductivity ratios ($k_r = k_p/k_f$) of 0.02, 1 and 50.

Equations (1)–(7) were solved by a control volume based finite difference formulation and by the SIMPLE calculation procedures, as described in detail by Patankar [18] and Le Quere *et al.* [19]. Detailed descriptions on the grid system and validation tests for the present study are given in ref. [20]. Consequently, only brief remarks are summarized below.

A non-uniform grid system was employed in the calculation domain. The grid system was, respectively, 57×36, 57×44, 57×47 and 57×50 for opening ratios (A_o) of 0, 1/8, 1/4 and 1/2. Checks were made by comparing the results from a 57×36 grid system with those from a 81×60 grid system, and agreements were very satisfactory. The presence of the partition plate in the calculation domain was accounted for by the strategy suggested by Patankar [21], in which equations (1)–(7) were solved for the entire domain and the partition plate was characterized by a region of very high viscosity (say, $\nu = 10^{30}$ m^2 s^{-1}) and a dimensionless partition conductivity k_r. The convergence criterion for each control volume was that the maximum residual of the mass, momentum and energy was less than 3.5×10^{-5}.

Prior to the calculations, checks were conducted to validate the calculation procedures by reference to the flow generated by differentially heating the side walls of a simple rectangular enclosure while keeping the top and bottom walls adiabatic. The results were in very good agreement with the benchmark solution of de Vahl Davis [22]. The accuracy of the calculation was also checked for an enclosure convection with an opening in the partition plate under differently uniform temperatures on the two side walls. The results, together with the measurement data of Chen *et al.* [16], are presented in Figs. 2 and 3, respectively, for the velocity and temperature profiles at various x-planes. It is seen that calculations predicted the thermal and fluid behaviours very well. For the present study, the computation time was approximately 2000–6000 s on a CDC CYBER 170/815 when $Ra^* = 10^4$–10^6, and was about 7000–9000 s when $Ra^* = 10^7$–10^8.

3. RESULTS AND DISCUSSIONS

3.1. *Velocity and temperature fields*

Figure 4 shows the vector velocity field and the isotherms for $Ra^* = 10^4$, 10^6 and 10^8 at $k_r = 1$ and $A_o = 0$ (no opening). It is seen from Fig. 4(a) that there is a clockwise recirculation zone in each half of the enclosure for $Ra^* = 10^4$, and the isotherms shown are nearly conduction like. Because the boundary layer has not developed at $Ra^* = 10^4$, so the fluid along the hot wall does not separate from the side wall and there appears no entrapment of the hot fluid. However, as Ra^* increases as shown in Figs. 4(b) and (c), the fluid along the hot wall separates at a height $y/H = 0.5$, while some fluid is trapped in the weak circulation zone in the upper and left quadrant. The separated fluid flows almost horizontally and turns around the bottom of the partition. It then flows along the partition plate to the top wall, makes a turn along the cold and bottom walls, and recirculates back to the hot wall. The flow patterns depicted for $Ra^* = 10^6$ and 10^8 are basically the same as those observed by Nansteel and Greif [10, 11]. It is also shown in Figs. 4(b) and (c) that as Ra^* increases, thermal boundary layers develop along the side walls and the thermal

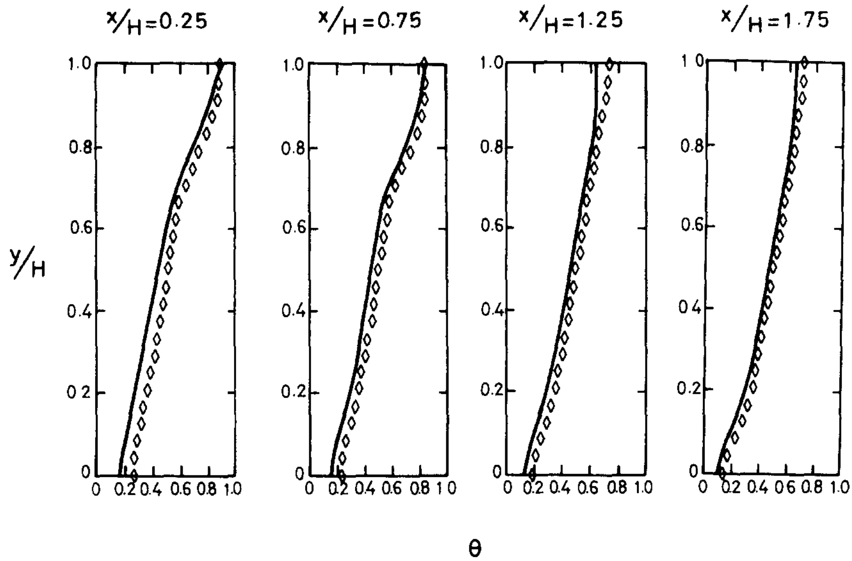

FIG. 3. Comparison of temperature profiles; ——, calculation; ◇, from ref. [16].

field away from the solid boundaries is essentially stratified. Because the conductivity ratio k_r is equal to unity (i.e. $k_f = k_p$, so the isotherms cross the partition plate smoothly.

The velocity vector field and the isotherms for $A_o = 1/8$, $1/4$ and $1/2$ are shown in Figs. 5(a)–(c) for $Ra^* = 10^4$ and $k_r = 1$. It is seen that with an opening in the partition plate, most of the hot fluid in the left quadrant flows through the opening; the remainder flows towards the bottom of the partition and makes a turn there. There still exists a clockwise circulation cell in each half of the enclosure, but its size is reduced. In addition, the isotherms (say, $\theta = 0.0$) elongate to the right-hand half of the enclosure and the heat transfer between the two halfs would be more effective. Figure 6 shows the velocity field and the isotherms for

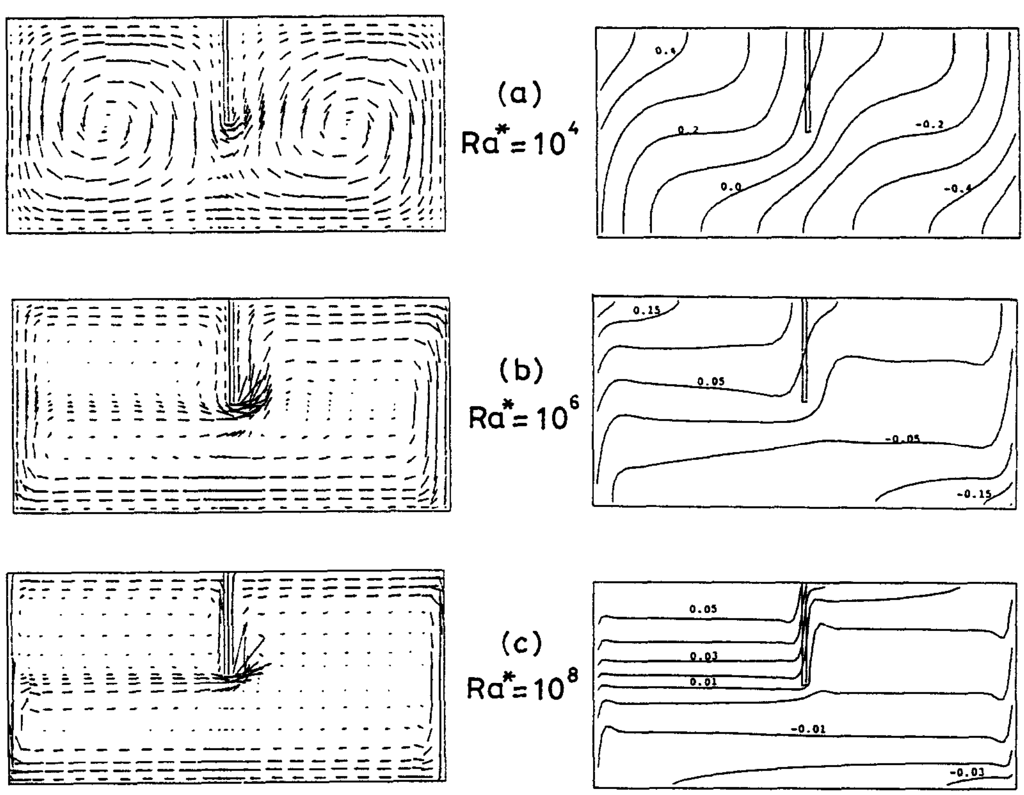

FIG. 4. Velocity vector field and isotherms for different Ra^* at $A_o = 0$ and $k_r = 1$.

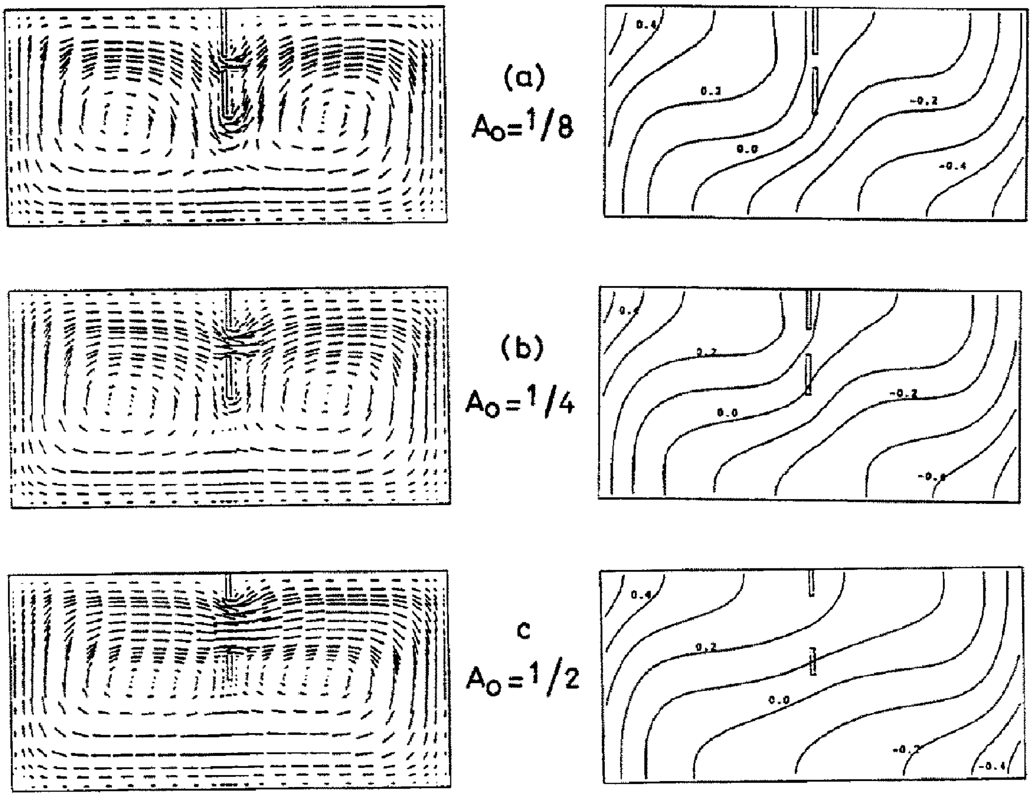

FIG. 5. Velocity vector field and isotherms for different A_o at $Ra^* = 10^4$ and $k_r = 1$.

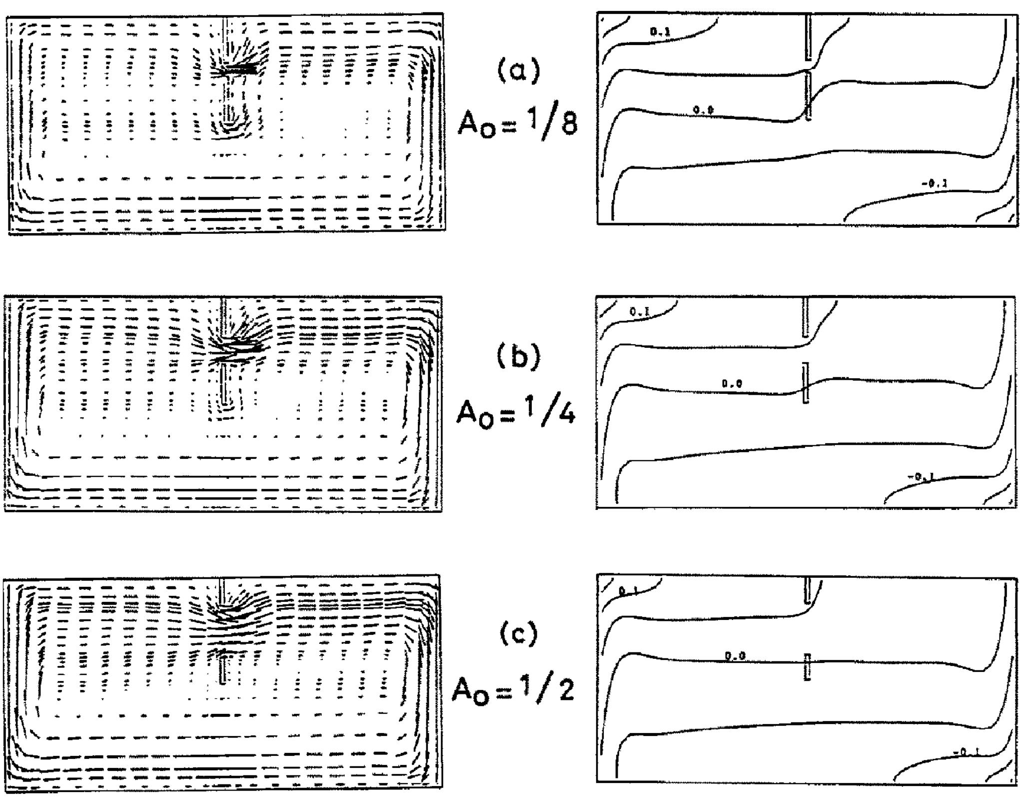

FIG. 6. Velocity vector field and isotherms for different A_o at $Ra^* = 10^6$ and $k_r = 1$.

$A_o = 1/8$, 1/4 and 1/2 at $Ra^* = 10^6$ and $k_r = 1$. It is seen that at higher Ra^* the circulation cell in the upper and left quadrant disappeared, and the fluid recirculated back mainly along the thin layers adjacent to the cold and bottom walls. These flow patterns are similar to the visualization results of ref. [16]. The isotherms (Figs. 5(a)–(c)) show clearly that the thermal field is essentially stratified with the thin boundary layers along the two side walls. That is, convection is the dominant heat transfer mechanism at high Ra^*.

The effect of the thermal conductivity of the partition plate on the thermal field is illustrated in Fig. 7 for three sets of conductivity ratios at $Ra^* = 10^7$ and $A_o = 1/8$. It is seen that for the case of an adiabatic partition (say, $k_r = 0.02$) some of the isotherms cannot reach out to the other side of the partition plate; but otherwise there does not seem to be any appreciable difference in the isotherm patterns. It was found numerically [20] that the effect of the partition conductivity was small and decreased as the opening ratio A_o increased.

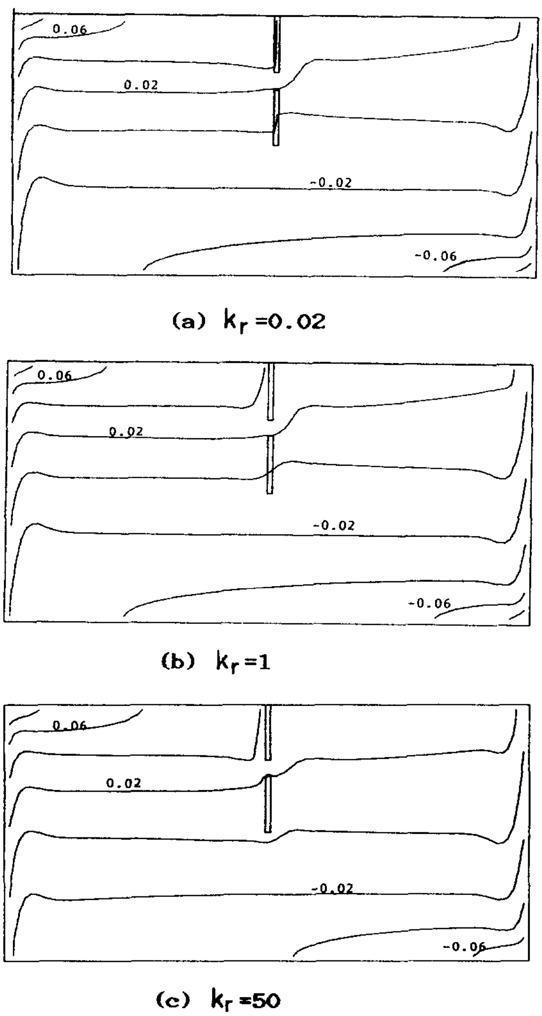

FIG. 7. Isotherms for different k_r at $Ra^* = 10^7$ and $A_o = 1/8$.

The vertical velocity profiles at the partition plane where $x/H = 1.0$ are shown in Figs. 8(a)–(d) for various Ra^* and A_o at $k_r = 1$. It is seen that the hot fluid flows to the right-hand side of the enclosure mainly through the bottom of the partition when $A_o = 0$ (no opening), but mainly through the opening when $A_o > 0$. The peak velocity of the right-moving flow is below the bottom of the partition when $A_o = 0$ and is in the middle of the opening when $A_o > 0$. However, the opening seems to have little effect on the velocity profiles of the left-moving flow near the bottom walls. Because convection is dominant at high Ra^*, so there appears a left-moving, boundary-type flow along the bottom wall for $A_o \geqslant 1/4$ and $Ra^* = 10^8$.

3.2. *Local Nusselt number distributions*

The local Nusselt number on the side walls is defined by

$$Nu_y = \frac{qH}{k_f(T_h - T_c)} \tag{8}$$

where T_h and T_c are, respectively, the temperatures of the hot (where $x/H = 0$) and cold (where $x/H = 2$) walls at location y. Since $\theta = (T - T_\infty)/(qH/k_f)$, it follows that

$$Nu_y = \frac{1}{\theta_h - \theta_c}. \tag{9}$$

That is, Nu_y is inversely proportional to the wall temperature difference at height y. The results of local Nusselt number distributions are shown in Figs. 9(a)–(d) for $10^4 \leqslant Ra^* \leqslant 10^8$ and $A_o = 0$, 1/4, 1/8 and 1/2. It is seen that for all opening ratios Nu_y increases with increasing Ra^*. When the modified Rayleigh number is small (say, $Ra^* = 10^4$), local Nusselt number is nearly constant. When $A_o = 0$, the maximum value of Nu_y is at $y/H = 0.33 \sim 0.4$ depending on Ra^*; and Nu_y at $y/H = 0$ is greater than that at $y/H = 1$ and is especially noticeable when $Ra^* \geqslant 10^6$.

With an opening in the partition plate as shown in Figs. 9(b)–(d), Nu_y distributions appear as parabolic lines with the maximum values at $y/H = 0.5 \sim 0.57$. However, at high Ra^*, the value of Nu_y in the middle portion changes little. For example, $Nu_y \simeq 22$ for $0.3 \simeq y/H \simeq 0.7$ when $Ra^* = 10^8$ and $A_o = 1/2$ (Fig. 9(d)).

3.3. *Average Nusselt number Nu*

The average Nusselt number is determined by

$$Nu = \frac{q}{k_r} \int_0^H \frac{H\,\mathrm{d}y}{T_h - T_c} = \int_0^1 Nu_y \,\mathrm{d}Y. \tag{10}$$

The results of the calculated Nu for $10^4 \leqslant Ra^* \leqslant 10^8$, $A_o = 0$, 1/8, 1/4 and 1/2, and $k_r = 0.02$, 1 and 50 are listed in Table 1. It is seen from Table 1 that Nu increases with increasing Ra^* and A_o. Although Nu also increases with increasing k_r, the effect is rather small as compared to the variation of k_r. For example, at $Ra^* = 10^6$ and $A_o = 1/8$, Nu is equal to 7.90 for

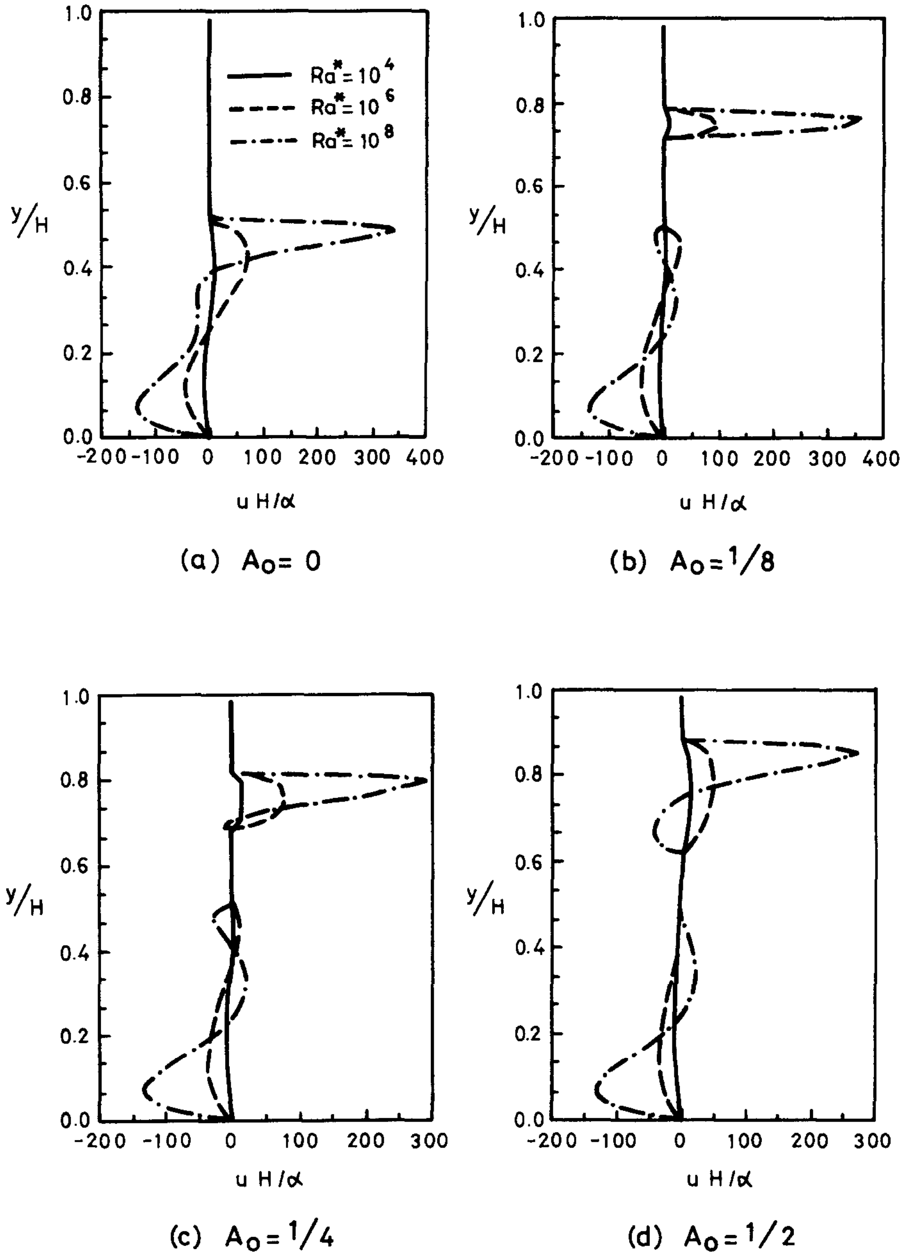

FIG. 8. Vertical velocity distributions at the partition plane ($x/H = 1.0$) at $k_r = 1.0$.

Table 1. Values of averaged Nusselt number, Nu

	K_r											
	$A_o = 0$			$A_o = 1/8$			$A_o = 1/4$			$A_o = 1/2$		
Ra^*	0.02	1	50	0.02	1	50	0.02	1	50	0.02	1	50
10^4	1.4	1.44	1.48	1.52	1.57	1.61	1.66	1.68	1.69	1.83	1.88	1.90
10^5	3.59	3.97	3.97	3.90	3.99	4.03	4.49	4.70	4.76	5.12	5.31	5.51
10^6	6.72	7.32	7.49	7.75	7.90	8.00	8.51	8.60	8.66	9.15	9.20	9.25
10^7	10.43	11.62	12.04	13.59	13.60	13.68	14.00	14.02	14.06	14.24	14.30	14.31
10^8	13.90	15.90	16.73	18.65	18.87	18.96	19.00	19.12	19.18	19.50	19.55	19.58

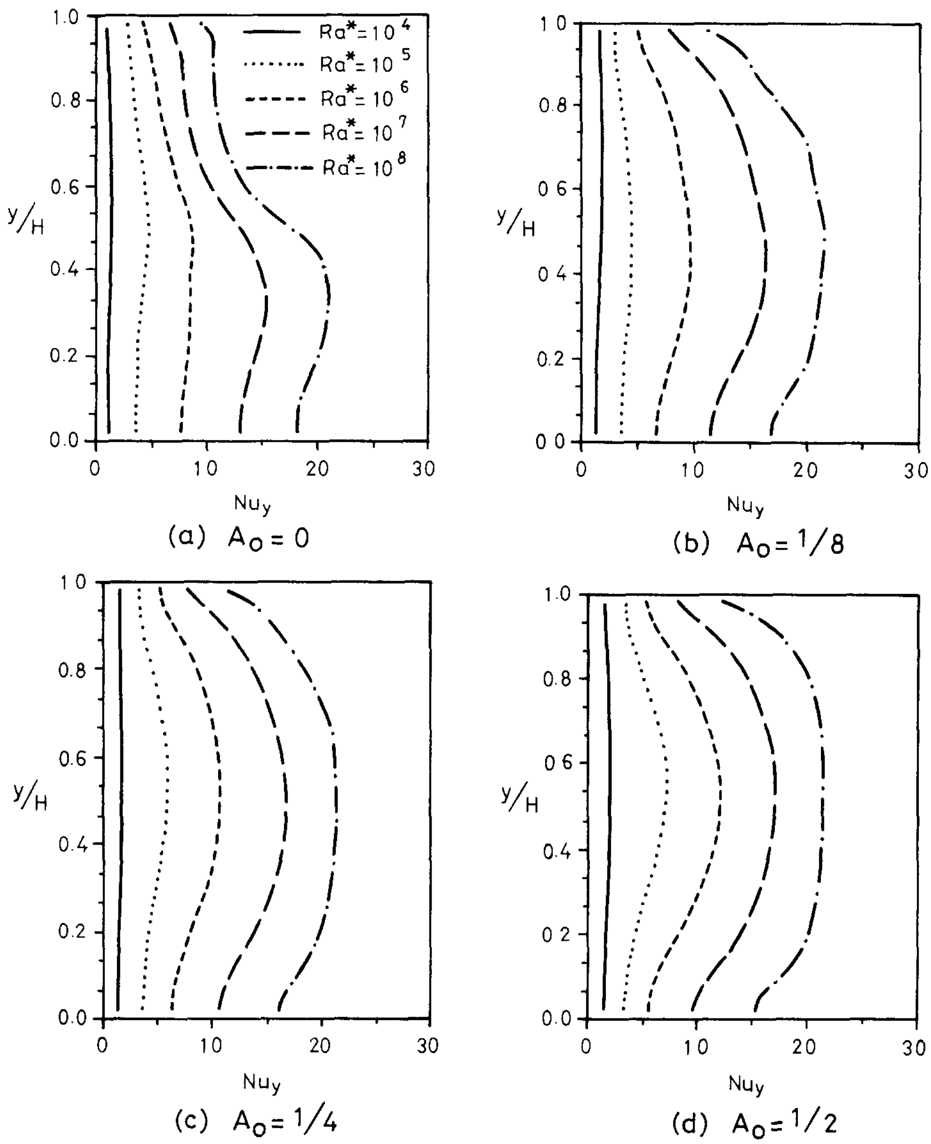

FIG. 9. Local Nusselt number distributions at $k_r = 1$.

$k_r = 1.0$, but is equal to 7.75 for $k_r = 0.02$ (adiabatic partition) and 8.0 for $k_r = 50$ (conducting partition); the variation is within $\pm 2\%$ of the value of Nu at $k_r = 1$ while for a 50 times variation of k_r. The negligible effect of k_r within the range of $0.02 \leqslant k_r \leqslant 50$ may be due to the fact that the partition thickness ratio is very small ($w/H = 0.01$) in this work.

Correlation of Nu as a function of Ra^* and A_o based on the values of Nu at $k_r = 1$ is given by

$$Nu = 0.176 Ra^{*0.258}(1-A_o)^{-0.328} \qquad (11)$$

for $10^4 \leqslant Ra^* \leqslant 10^8$, $0 \leqslant A_o \leqslant 1/2$, $0.02 \leqslant k_r \leqslant 50$ and $Pr = 7$. The above equation is shown as the solid lines in Fig. 10 for four different values of A_o. The r.m.s. deviation between the correlation equation and the calculated data is within 22%. It is obvious that the effect of k_r on Nu is negligible as compared with the scatter of the data. The dashed line in Fig. 10 is the correlation equation for a non-partitioned enclosure

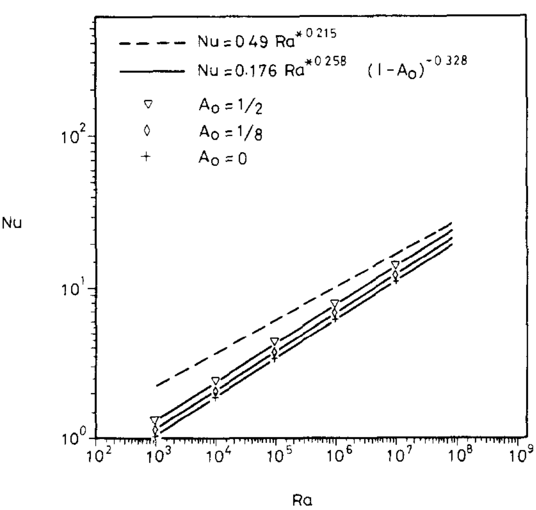

FIG. 10. Correlation of average Nusselt number.

($A_p = 0$) obtained in this study and is given by

$$Nu = 0.49Ra^{*0.215} \quad (12)$$

for $10^4 \leqslant Ra^* \leqslant 10^8$, $A = 2$ and $Pr = 7$. It is seen that an unopened partial obstruction would reduce the heat transfer rate by an amount of 12–44% depending on Ra^*.

4. SUMMARY

A numerical study is presented for natural convection in a two-dimensional, partially-divided, rectangular enclosure in which two side walls were maintained at uniform heat flux condition and the top and bottom walls were insulated. Results show that an unopened partial obstruction would reduce the heat transfer rate by an amount of 12–44% depending on Ra^*. An opening in the partition plate would increase the heat transfer rate by allowing the flow of the entrapped hot fluid (that would exist in an unopened, partially-divided, enclosure) through the opening. For the range studied in this work, the effect of partition conductivity on the heat transfer rate was rather small and could be neglected. A correlation of the Nusselt number is given which shows that the heat transfer rate increases with increasing modified Rayleigh number and opening ratio. It should be noticed that the effects of A_p and the partition width on the thermal and fluid characteristics need further study.

Acknowledgements—This work was partially supported by National Science Council in Taiwan under Grant NSC-75-0401-E110-01.

REFERENCES

1. I. Catton, Natural convection in enclosures, *Proc. 6th Int. Heat Transfer Conf.*, Toronto, Vol. 6, pp. 13–31 (1978).
2. A. Bejan, *Convection Heat Transfer*, pp. 159–201. Wiley, New York (1985).
3. K. T. Yang and J. R. Lloyd, *Proc. Workshop Natural Convection*, Colorado, 18–21 July (1982).
4. P. G. Simpkins and K. S. Chen, Natural convection in horizontal containers with application to crystal growth. In *Natural Convection: Fundamentals and Applications* (Edited by S. Kakac, W. Aung and R. Viskanta), pp. 1010–1039. Hemisphere, Washington, DC (1985).
5. A. F. Emery, Exploratory studies of free convection heat transfer through an enclosed vertical liquid layer with a vertical baffle, *ASME J. Heat Transfer* **19**, 163–165 (1969).
6. F. Bauman, A. Gagil, R. Kammerud and R. Greif, Buoyancy driven convection in rectangular enclosures: experimental results and numerical calculations, ASME 80-HT-66 (1980).
7. L. C. Chang, J. R. Lloyd and K. T. Yang, A finite difference study of natural convection in complex enclosures, *Proc. 7th Int. Heat Transfer Conf.*, Munich, Federal Republic of Germany, pp. 183–188 (1982).
8. H. E. Janikowski, J. Ward and S. D. Probert, Free convection in vertical air-filled rectangular cavities fitted with baffles, *Proc. 6th Int. Heat Transfer Conf.*, Toronto, Vol. 6, pp. 257–262 (1978).
9. S. M. Bajorek and J. R. Lloyd, Experimental investigation of natural convection in partitioned enclosures, *ASME J. Heat Transfer* **104**, 527–532 (1982).
10. W. M. Nansteel and R. Greif, Natural convection in undivided and partially divided rectangular enclosures, *ASME J. Heat Transfer* **103**, 623–629 (1981).
11. W. M. Nansteel and R. Greif, An investigation of natural convection in enclosures with two- and three-dimensional partitions, *Int. J. Heat Mass Transfer* **27**, 561–571 (1984).
12. N. N. Lin and A. Bejan, Natural convection in a partially divided enclosure, *Int. J. Heat Mass Transfer* **26**, 1867–1878 (1983).
13. R. Jetli, S. Acharya and E. Zimmerman, Influence of baffle location on natural convection in a partially divided enclosure, *Numer. Heat Transfer* **10**, 521-536 (1986).
14. H. J. Shaw, C. K. Chen and J. W. Cleaver, Cubic spline numerical solution for two-dimensional natural convection in a partially divided enclosure, *Numer. Heat Transfer* **12**, 439–455 (1987).
15. E. Zimmerman and S. Acharya, Free convection heat transfer in a partially divided vertical enclosure with conducting end walls, *Int. J. Heat Mass Transfer* **30**, 319–331 (1987).
16. K. S. Chen, A. C. Ku and C. H. Chou, Investigation of natural convection in partially divided rectangular enclosures both with and without an opening in the partition plate, *ASME J Heat Transfer* **112**, 648–652 (1990).
17. S. Kimura and A. Bejan, The boundary layer natural convection regime in a rectangular cavity with uniform heat flux from the side, *ASME J. Heat Transfer* **106**, 98–106 (1984).
18. S. V. Patankar, *Numerical Heat Transfer and Fluid Flow*. McGraw-Hill, New York (1980).
19. P. Le Quere, J. A. C. Humphrey and F. S. Sherman, Numerical calculation of thermally driven two-dimensional unsteady laminar flow in cavities of rectangular cross section, *Numer. Heat Transfer* **4**, 249–283 (1981).
20. P. W. Ko, Numerical simulation of natural convection in rectangular enclosures partially divided by conducting plates, M.S. thesis, Inst. of Mech. Engng, National Sun Yat-Sen Univ., Kaohsiung, Taiwan (1989).
21. S. V. Patankar, A numerical method for conduction in composite materials, flow in irregular geometries and conjugate heat transfer, *Proc. 6th Int. Heat. Transfer Conf.*, Toronto, Vol. 3, p. 297 (1978).
22. G. de Vahl Davis, Natural convection of air in a square cavity: an accurate numerical solution, Report 1981/FMT/1, University of N.S.W., Kensington, Australia (1981).

CONVECTION NATURELLE DANS UNE ENCEINTE RECTANGULAIRE PARTIELLEMENT DIVISEE AVEC UNE OUVERTURE DANS LA PLAQUE DE PARTITION ET LES PAROIS LATERALES ISOFLUX

Résumé—On présente une étude numérique de la convection naturelle dans une enceinte bidimensionnelle, rectangulaire, partiellement divisée dans laquelle deux parois latérales sont soumises à une condition de flux uniforme et les parois supérieure et inférieure sont isolées. Le nombre de Rayleigh modifié varie de 10^4 à 10^8; les rapports d'ouverture 0, 1/4, 1/8 et 1/2 et les rapports de conductivité 0,02, 1 et 50 sont choisis pour un rapport de forme (longueur/hauteur) de 2, un rapport de partition de 1/2 et un nombre de Prandtl de 7 (eau). Les résultats montrent que le fluide chaud se déplace vers l'autre côté de la cavité, principalement par le bas de la partition quand il n'y a pas d'ouverture dans la cloison, et une zone de faible circulation est présente dans le quadrant supérieur gauche. Avec une ouverture dans la partition, la plupart du fluide s'écoule vers l'autre côté à travers l'ouverture et la zone de circulation dans le cadrant supérieur gauche est réduite en taille ou disparaît. L'effet de la conductivité de la partition sur le transiert de chaleur est plutôt faible et il peut être négligé. On obtient et discute une formule du nombre de Nusselt moyen en fonction du nombre de Rayleigh modifié et du rapport d'ouverture. Les résultats montrent aussi qu'une obstruction partielle peut réduire le transfert de chaleur de 12–44% selon le nombre de Rayleigh modifié.

NATÜRLICHE KONVEKTION IN EINEM PARTIELL UNTERTEILTEN RECHTECKIGEN HOHLRAUM MIT EINER ÖFFNUNG DER TRENNWAND UND GLEICHMÄSSIG BEHEIZTEN SEITENWÄNDEN

Zusammenfassung—Die natürliche Konvektion in einem zweidimensionalen partiell unterteilten rechteckigen Hohlraum, bei dem zwei Seitenwände gleichförmig beheizt werden während die obere und untere Deckfläche adiabat sind, wird numerisch untersucht. Die modifizierte Rayleigh-Zahl liegt zwischen 10^4 und 10^8, die Öffnungsverhältnisse betragen 0; 1/4; 1/8 und 1/2, die Leitfähigkeitsverhältnisse 0,02; 1 und 50 während das Seitenverhältnis (Länge/Höhe) 2, das Flächenverhältnis der Unterteilung 1/2 und die Prandtl-Zahl 7 (Wasser) beträgt. Die Ergebnisse zeigen, daß das heiße Fluid vornehmlich durch den unteren Teil der Trennwand auf die andere Seite des Hohlraums strömt, wenn keine Öffnung in der Trennwand ist. Im oberen linken Quadranten ergibt sich eine schwache Zirkulationszone. Befindet sich eine Öffnung in der Trennwand, so strömt das meiste Fluid durch diese Öffnung auf die andere Seite und die Zirkulationszone im oberen linken Quadranten verkleinert sich oder verschwindet gänzlich. Der Einfluß der Wärmeleitfähigkeit der Trennwand auf den Wärmeübergang erweist sich als vernachlässigbar klein. Es wird eine Korrelationsgleichung für die mittlere Nusselt-Zahl in Abhängigkeit von der modifizierten Rayleigh-Zahl und vom Öffnungsverhältnis ermittelt und diskutiert. Die Ergebnisse zeigen, daß eine nichtgeöffnete partielle Trennwand den Wärmeübergang um 12–44% reduziert—je nach Höhe der modifizierten Rayleigh-Zahl.

ЕСТЕСТВЕННАЯ КОНВЕКЦИЯ В ЧАСТИЧНО ПЕРЕГОРОЖЕННОЙ ПРЯМОУГОЛЬНОЙ ПОЛОСТИ С ОТВЕРСТИЕМ В РАЗДЕЛЯЮЩЕЙ ПЛАСТИНЕ И ИЗОТЕРМИЧЕСКИМИ БОКОВЫМИ СТЕНКАМИ

Аннотация—Численно исследуется естественная конвекция в двумерной частично перегороженной прямоугольной полости, на боковых стенках которой поддерживается однородный тепловой поток, а верхние и нижние стенки изолированы. Исследования проводились для модифицированного числа Рэлея, изменяющегося в диапазоне 10^4–10^8, отношения отверстий, составляющих 0, 1/4, 1/8, и 1/2, а также для отношения теплопроводностей, равного 0,02; 1 и 50 и отношения длины полости к высоте, составляющего 2, отношения размеров перегородки, равного 1/2, значения числа Прандтля, равного 7 (вода). Результаты показывают, что нагретая жидкость перетекает к противоположной стороне полости в основном через нижнюю часть перегородки в случае отсутствия в ней отверстий и что в верхнем левом квадранте существует зона слабой циркуляции. При наличии отверстия в перегородке большая часть жидкости перетекает к противоположной стороне полости через него, а циркуляционная зона в верхнем левом квадранте уменьшается в размере и исчезает. Найдено, что влияние теплопроводности перегородки на интенсивность теплопереноса достаточно мало и может не учитываться. Выводится и обсуждается обобщенное соотношение для среднего числа Нуссельта, выраженное через модифицированное число Рэлея и отношение размеров отверстий. Полученные результаты также показывают, что частичная перегородка без отверстий приводит к снижению интенсивности теплопереноса на 12–44% в зависимости от значения модифицированного числа Рэлея.